INSTITUTE OF PHYSICS PUBLISHING JOURNAL OF PHYSICS D: APPLIED PHYSICS

J. Phys. D: Appl. Phys. **35** (2002) 2243–2246 PII: S0022-3727(02)37155-9

Growth of $SrRuO_3$ thin films on MgO substrates by pulsed laser ablation

S K Singh[1,2], M R Lees[1], R K Singh[2] and S B Palmer[1]

[1] Department of Physics, University of Warwick, Coventry CV4 7AL, UK
[2] School of Pure and Applied Physics, Guru Ghasidas University, Bilaspur-495009, India

Received 20 May 2002, in final form 25 July 2002
Published 4 September 2002
Online at stacks.iop.org/JPhysD/35/2243

Abstract

$SrRuO_3$ thin films have been grown on MgO substrates using pulsed laser ablation deposition. The orientation of the $SrRuO_3$ films changes from the [001] or [110] direction normal to the substrate surface to become predominantly [100] as the thickness of the $SrRuO_3$increases from 50 to 360 nm. This leads to a change in the magnetic response of the $SrRuO_3$ films and to a dramatic improvement in the superconducting properties of $YBa_2Cu_3O_{7-\delta}$ films grown on top of the $SrRuO_3$ layer. The domain structures and the surface morphology of $SrRuO_3$ films grown on MgO change as the thickness of the film increases. The 50 nm thick $SrRuO_3$ film grown on an MgO substrate nucleates as rectangular islands, 0.5 to 1 μm in diameter. As the thickness increases to 185 nm, oriented grains $\sim$1 μm in size are observed. We have noted a different microstructure for the $SrRuO_3$ thin films grown on $SrTiO_3$ substrates. The 185 nm thick $SrRuO_3$ film grown on a $SrTiO_3$ substrate shows a step like growth pattern.

1. Introduction

Thin films of $SrRuO_3$ have received continuous attention for more than ten years due to their useful electronic, magnetic and optical properties. Epitaxial thin films and heterostructures based on $SrRuO_3$ may be important in the development of many different types of devices including those based on spin-polarized tunnel junctions. $SrRuO_3$ is a conductive magnetic oxide, which is paramagnetic at room temperature and ferromagnetic below 160 K [1, 2]. At room temperature, $SrRuO_3$ has an orthorhombic structure with the space group of Pbnm and lattice parameters $a = 5.5670$ Å, $b = 5.5304$ Å and $c = 7.8446$ Å [3]. Its relatively high remanent magnetization and large magneto-optical constant make it potentially attractive for various electronic and optical devices [4]. More fundamental issues such as interface physics and growth mechanisms of artificial structures are also important for device fabrication [5, 6]. In order to study the physics of spin-polarized tunnel junction devices, a sharp interface and defect-free barrier layer in the multilayered tunnel junctions are required. The properties of this barrier must be controlled on an atomic scale [7]. $SrRuO_3$ is an ideal bottom electrode in devices incorporating oriented ferroelectric films, due to its relatively high thermal conductivity, and good compatibility in structure and chemistry with perovskite type ferroelectric materials. Ferroelectric capacitors with $SrRuO_3$ thin film electrodes for non-volatile memory, exhibit superior fatigue and leakage characteristics [8–11]. Such devices are sensitive to the surface morphology and microstructure of the thin films. Surface morphology, domain structure and growth mechanisms can be controlled by the lattice mismatch between the substrate and the film [12]. The surface morphology and chemistry of the substrate can be modified by surface treatments including annealing or chemical etching of the substrate allowing the growth of epitaxial thin films [13–15]. It is generally believed that a miscut substrate changes the growth mechanisms of $SrRuO_3$ thin films, which can in turn lead to changes in their electrical transport and magnetic behaviour [16]. When $SrRuO_3$ is deposited on a (001) $SrTiO_3$ substrate, the film can grow epitaxially with either the [001] or the [110] direction normal to the $SrTiO_3$ surface [17]. The $SrRuO_3$ films grown on (001) $SrTiO_3$ show two types of [110] domains [18–20]. The domain structures and the surface morphology of $SrRuO_3$ films grown on $LaAlO_3$ substrates are different from those grown on $SrTiO_3$. The rougher surface produced on $LaAlO_3$ is due to a lattice mismatch across the film/substrate interface [21].

Due to a good lattice match[3], the majority of epitaxial $SrRuO_3$ thin films have been grown on $SrTiO_3$ or $LaAlO_3$ single-crystal substrates. Various deposition methods, such as 90° off-axis sputtering [19, 22], MBE [23], laser MBE [24, 25] and pulsed laser ablation [26] have been used. Growth on Si substrates requires a buffer layer of suitable material such as yttria stabilized zirconia, due to the high chemical reactivity between Si and $SrRuO_3$ [27]. There have been no reports of the growth of $SrRuO_3$ on MgO. MgO substrates are an attractive option because they are inexpensive and are readily available with an area of at least $20 \times 20\,mm^2$. The lattice mismatch between $SrRuO_3$ and the MgO substrate, however, is about 7.1%. In this work, we have grown $SrRuO_3$ thin films of different thicknesses on MgO substrates. We have investigated whether it is possible to grow good quality thin films of $SrRuO_3$ on this substrate material. We have studied the growth mechanism and morphology of these films. We show that there are interesting changes in the film structure as the $SrRuO_3$ film thickness is increased. For comparison we have also grown films on $SrTiO_3$ under the same deposition conditions. Finally, we have grown $SrRuO_3/YBa_2Cu_3O_{7-\delta}$ bilayers to demonstrate the effects the changes in the properties of the $SrRuO_3$ layers have on properties of the bilayer structures.

2. Experimental details

All the $SrRuO_3$ thin films and $SrRuO_3/YBa_2Cu_3O_{7-\delta}$ bilayers have been grown on MgO or $SrTiO_3$ substrates by pulsed laser ablation deposition. A XeCl excimer laser that produces UV radiation of wavelength 308 nm was used. During growth, the targets were rotated and the laser beam was scanned across the target surface to minimize degradation [28]. The laser irradiance at the target was fixed at $1.8\,J\,cm^{-2}$ with a pulse repetition rate of 10 Hz. The sample chamber was evacuated to 10^{-6} mbar prior to the deposition of the films. The films were deposited in oxygen at an operating pressure of 0.2–0.3 mbar and a temperature of 700–770°C. After deposition, the films were cooled down to 450°C in an oxygen pressure of 200 mbar and then held at 450°C for 15 min and then finally cooled to room temperature. We have obtained $SrRuO_3$ films with different thicknesses by changing only the deposition time, keeping all the other growth conditions fixed.

Film stoichiometry and orientation were determined by x-ray diffraction using CuKα radiation. The chemical homogeneity of the films was investigated using energy dispersive x-ray analysis (EDAX). The thickness (t) of the films was measured *ex situ* with a stylus instrument. The surface morphology of the films was investigated using a Burleigh atomic force microscope (AFM) operating in the contact mode. DC resistivity measurements were made in a closed-cycle cryostat using a standard four-probe method. Silver wires were attached to each film using silver paste. Currents of between 10^{-5} and 10^{-6} A were injected into the plane of the films. The voltage was measured using a nanovoltmeter. The magnetic measurements were performed using a Quantum Design SQUID magnetometer operating in the DC measurement mode.

[3] There is a lattice mismatch of about 0.64% between $SrRuO_3$ and a $SrTiO_3$ substrate. $SrTiO_3$ has a cubic perovskite structure with a lattice constant of 3.905 Å at a deposition temperature of 650°C.

3. Results and discussion

Several films of $SrRuO_3$ with thickness t between 50 and 360 nm were grown. $YBa_2Cu_3O_{7-\delta}$ (YBCO) layers of thickness 25–30 nm were then grown on the $SrRuO_3$ buffer. The orientation of the films was investigated using x-ray diffraction. In the case of the $SrRuO_3$ films grown on MgO substrates, the strongest peaks in the spectra of the thinnest film ($t = 50$ nm) can be indexed as $(l, l, 0)$ or $(0, 0, l)$ peaks. Because of the systematic absence of the $(0, 0, l)$ peaks, where l is odd, and the near degeneracy of d_{110} and d_{002} in $SrRuO_3$ (d is the inter planar spacing), it is not possible to distinguish between these two textures using a simple 2θ scan [22]. As t increases, the peaks corresponding to $(l, 0, 0)$ increase in intensity suggesting a-axis alignment. Figure 1 shows the ratio of the intensities of the (200) and (004) peaks, $I_{(200)}/I_{(004)}$, as a function of film thickness. Initially $SrRuO_3$ grows with the [001] or [110] direction normal to the substrate; then, as t increases, growth takes place with the [100] direction perpendicular to the plane of the film. An a-axis alignment has also been reported for films of thickness between 100 and 300 nm grown on $LaAlO_3$ and $SrTiO_3$ substrates [4, 29]. The $SrRuO_3$ films deposited on $SrTiO_3$ (001) substrates show high intensity $SrRuO_3$ peaks corresponding to the $(0, 0, 2l)$ reflections for all thicknesses. All the YBCO films grow as c-axis textured films.

The surface morphology of the thin films was investigated using an AFM. The 50 nm thick $SrRuO_3$ films have a root mean square (rms) surface roughness of 0.01 μm over a scan area of $7 \times 7\,\mu m^2$. The roughness of the films increases with the film thickness, and the 185 nm thick film has a rms roughness of 0.04 μm over the same scan area. EDAX measurements show that all the films are stoichiometric to within the accuracy of our instrumentation[4]. Figure 2(a) shows the 50 nm thick $SrRuO_3$ film grown on an MgO substrate nucleating as rectangular islands, 0.5–1 μm in diameter, growing in random orientations due to the lattice mismatch. During growth, the build up of stress can be offset by the formation of misfit dislocations. The films also show spiral growth patterns indicating screw-dislocation mediated growth. *In situ* TEM studies by Jiang and Pan [21] have shown that $SrRuO_3$ has a cubic structure at the deposition temperature used and during the phase transition to the low temperature orthorhombic phase, the formation of orientated domains can release elastic strain within the films. As the film thickness is increased to 185 nm the regions between neighbouring misfit dislocations become unstressed and the growth appears to be dominated by the fast growth nucleation. At a film thickness of 185 nm clearly oriented grains were observed as shown in figure 2(b). Figure 3 shows the surface morphology of the 185 nm thick $SrRuO_3$ film grown on the $SrTiO_3$ substrate and reveals a periodic step pattern with straight steps, suggesting a step flow growth as previously reported [7, 16].

Magnetization versus temperature measurements indicate that all the $SrRuO_3$films order ferromagnetically with an ordering temperature, T_{FM}, of 160 K. Magnetization versus field loops were taken to investigate the magnetic properties of the $SrRuO_3$ layers with the applied field in the plane of the substrate. Data taken at 5 K, which is typical of the curves

[4] The Sr/Ru ratio is 1 : 1 to within ±5%.

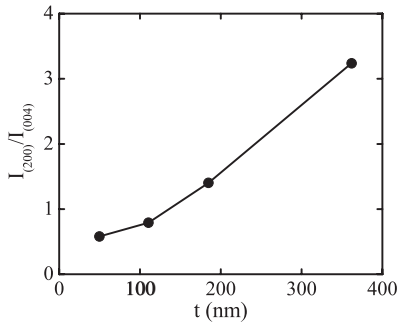

Figure 1. The ratio of the x-ray peak intensities I of the (200) and the (220)/(004) peaks as a function of film thickness (t) for $SrRuO_3$ thin films grown on MgO substrates. $I_{(200)}/I_{(004)}$ increases rapidly indicating a chang in film orientation with thickness.

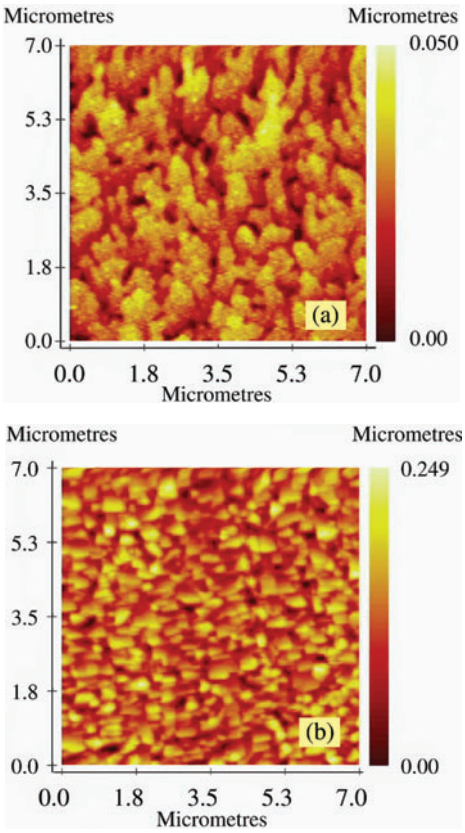

Figure 2. AFM images of $SrRuO_3$ films of different thickness grown on MgO substrates (*a*) 50 nm thick and (*b*) 185 nm thick. As the thickness of $SrRuO_3$ increases from 50 to 185 nm clearly oriented grains are observed.

collected, is shown in figure 4. The data has been corrected to remove a diamagnetic contribution from the substrate material. By measuring the film thickness and area and using the published value for the density of $SrRuO_3$ [3] we have estimated the mass of material present. The magnetization signals do not saturate in fields of up to 50 kOe. Both the remanent magnetization and the coercive field increase with film thickness. The magnitude of the signal at 50 kOe decreases with increasing film thickness and corresponds to a moment of 0.55 μ_B Ru^{-1} for a film thickness t of 360 nm and 1.1 μ_B Ru^{-1} for $t = 50$ nm. The higher value matches the published value for the saturation

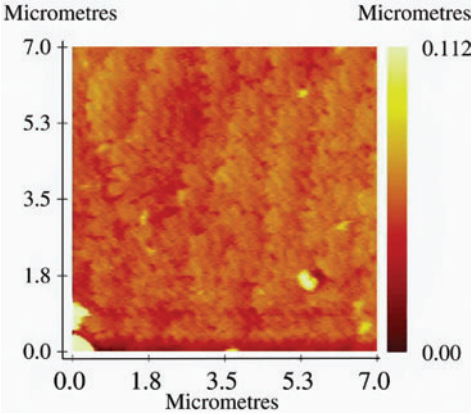

Figure 3. AFM image of a 185 nm thick $SrRuO_3$ film grown on $SrTiO_3$ substrate. The image shows the step growth pattern.

moment along the [110] easy axis in $SrRuO_3$ single crystals [30]. These observations are consistent with a change in alignment of the $SrRuO_3$ films as the film thickness t increases, with the easy axis rotating out of the plane.

Figure 5 presents the electrical resistivity versus temperature of the $SrRuO_3$/YBCO layers. The electrical resistivity of the $SrRuO_3$ films prior to deposition of the final YBCO layer demonstrate the expected behaviour. There is linear ρ–T behaviour above T_{FM} and a kink at 160 K indicating a decrease in magnetic scattering with the onset of long-range ferromagnetic order [31]. The ρ–T measurements of films after deposition of the YBCO layer contain several features, which should be noted. There is a systematic decrease in the resistivity of the bilayers as the thickness of the $SrRuO_3$ layer increases. This is not unexpected since the metallic $SrRuO_3$ may carry a portion of the current in the normal state leading to an overall decrease in resistivity with increasing thickness. However, the kink in the data around 160 K becomes less evident as the thickness of the $SrRuO_3$ layer increases. Since all the YBCO layers are nominally of the same thickness, this cannot be explained by a change in the form factor of the YBCO and is not consistent with the thicker $SrRuO_3$ layers carrying a greater proportion of the current. We suggest that as the thickness of the $SrRuO_3$ increases and the layers become oriented with the [100] direction perpendicular to the plane of the substrate, the quality of the YBCO layer improves, due to a combination of a good lattice match between the $SrRuO_3$ and the YBCO (see [32][5]) and an improved in plane grain alignment in the $SrRuO_3$ (see figure 2). This is supported by the behaviour observed around the superconducting transition temperature T_C. As the thickness t increases, T_C (onset) increases from 75 to 92.5 K. The width of the transition decreases from 15 to 3 K and the tail present in the data for the film grown on the 50 nm layer disappears.

4. Summary

We have shown that as the thickness of the $SrRuO_3$ increases from 50 to 360 nm, the orientation of the $SrRuO_3$ films on

[5] For the thicker *a*-axis oriented $SrRuO_3$ we suggest there may be domain-matching epitaxial growth of the YBCO layer.

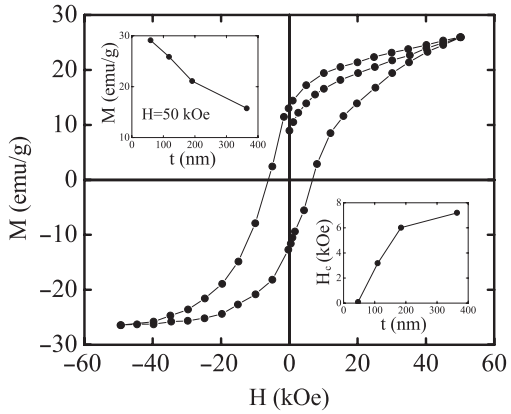

Figure 4. Magnetization as a function of magnetic field for a $t = 110$ nm $SrRuO_3$ film at 5 K. The insets show the coercive field (H_C) versus thickness (t) and magnetization (M) in a magnetic field of 50 kOe versus thickness (t) for $SrRuO_3$ thin films grown on MgO substrates.

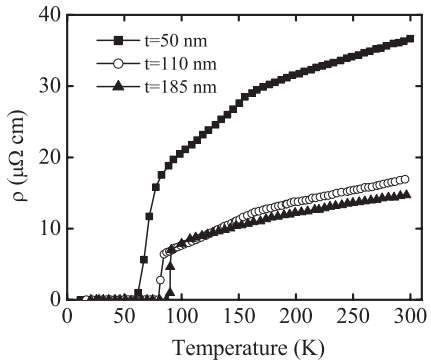

Figure 5. Electrical resistivity as a function of temperature for three $SrRuO_3$/YBCO bilayers grown on MgO substrates, each with a different thickness (t) of $SrRuO_3$ and the same thickness of YBCO. As the thickness (t) increases and the orientation of the $SrRuO_3$ buffer layer changes, the normal and superconducting properties of the YBCO layer improve.

MgO substrates changes from a state where the [001] or [110] direction lies normal to the substrate surface, to a situation where the [100] direction is perpendicular to the plane of the film. This leads to a change in the magnetic response of the $SrRuO_3$ films. Initially the $SrRuO_3$ films on a MgO substrate nucleate as rectangular islands growing in all possible directions, which merge together to form oriented grains as the thickness increases. YBCO layers of thickness 25–30 nm were then grown on the $SrRuO_3$ buffer. As the thickness of the buffer layer of $SrRuO_3$ increases from 50 to 360 nm, a dramatic improvement in the superconducting properties of the YBCO thin films is observed. The YBCO films grown on thicker $SrRuO_3$ layers have a much higher T_C ($T_C = 92.5$ K for $t = 185$ nm). We suggest that as the thickness of the $SrRuO_3$ increases and the layers become oriented with the [100] direction perpendicular to the plane of the substrate, the quality of the YBCO layer improves.

Acknowledgments

One of the authors (SKS) wishes to acknowledge the Association of Commonwealth Universities for the award of a Commonwealth teacher fellowship. The authors wish to thank Mr Steve York for experimental support.

References

[1] Bouchard R J and Gillson J L 1972 *Mater. Res. Bull.* **7** 893
[2] Callaghan A, Moller C W and Ward R 1966 *Inorg. Chem.* **5** 1572
[3] Jones C W, Battle P D, Lightfoot P and Harrison W T A 1989 *Acta Crystallogr. Sect. C: Cryst. Struct. Commun.* C **45** 365
[4] Klein L, Dodge J S, Geballe T H, Kapitulnik A, Marshall A F, Antognazza L and Char K 1995 *Appl. Phys. Lett.* **66** 2427
[5] Wu M K, Ashburn L R, Torng C J, Hor P H, Meng R L, Gao L, Huang Z J, Wang Y Q and Chu C W 1987 *Phys. Rev. Lett.* **58** 908
[6] Sheng Z Z and Hermann A M 1988 *Nature* (London) **332** 138
[7] Choi J, Eom C B, Rijnders G, Rogalla H and Blank D H A 2001 *Appl. Phys. Lett.* **79** 1447
[8] Eom C B, Van Dover R B, Phillips J M, Werder D J, Marshall J H, Chen C H, Cava R J, Fleming R M and Fork D K 1993 *Appl. Phys. Lett.* **63** 2570
[9] Liu Z G, Yin J and Wu Z C 1999 *Appl. Phys.* A **69** S659
[10] Cheng H F, Ling Y C and Lin I N 2001 *Japan. J. Appl. Phys.* **40** 234
[11] Guerrero C, Roldan J, Ferrater C, Garcia-Cuenca M V, Sanchez F and Varela M 2001 *Solid-State Electron.* **45** 1433
[12] Kawasaki M, Takahashi K, Maeda T, Tsuchiya R, Shinohara M, Ishiyama O, Yonezawa T, Yoshimoto M and Koinuma H 1994 *Science* **266** 1540
[13] Jiang Q D and Zegenhagen J 1995 *Surf. Sci.* **338** L882
[14] Kawasaki M, Ohtomo A, Arakane T, Takahashi K, Yoshimoto M and Koinuma H 1996 *Appl. Surf. Sci.* **107** 102
[15] Koster G, Kropman B L, Rijnders G J H M, Blank D H A and Rogalla H 1998 *Appl. Phys. Lett.* **73** 2920
[16] Rao R A, Gan Q and Eom C B 1997 *Appl. Phys. Lett.* **71** 1171
[17] Jiang J C, Pan X Q and Chen C L 1998 *Appl. Phys. Lett.* **72** 900
[18] Jiang J C, Tian W, Pan X, Gan Q and Eom C B 1998 *Mater. Sci. Eng.* B **56** 152
[19] Gan Q, Roa R A, Eom C B, Wu L and Tsui F 1999 *J. Appl. Phys.* **85** 5297
[20] Kim S S, Kang T S and Je J H 2001 *J. Appl. Phys.* **90** 4407
[21] Jiang J C and Pan X Q 2001 *J. Appl. Phys.* **89** 6365
[22] Eom C B, Cava R J, Fleming R M, Phillips J M, Van Dover R B, Marshall J H, Hsu J W P, Krajewski J J and Fork D K 1992 *Science* **258** 1766
[23] Naito M, Yamamoto H and Sato H 1998 *Physica* C **305** 233
[24] Lippmaa M, Nakagawa N, Kawasaki M, Ohashi S, Inaguma Y, Itoh M and Koinuma H 1999 *Appl. Phys. Lett.* **74** 3543
[25] Lippmaa M, Nakagawa N, Kawasaki M, Ohashi S and Koinuma H 2000 *Appl. Phys. Lett.* **76** 2439
[26] Koster G, Rijnders G J H M, Blank D H A and Rogalla H 1999 *Appl. Phys. Lett.* **74** 3729
[27] Watanabe K, Ami M and Tanaka M 1996 *Mater. Res. Bull.* **32** 83
[28] Jackson T J, Appleyard N J, Copper M, Richards D H and Palmer S B 1995 *Meas. Sci. Technol.* **6** 128
[29] Lu P, Chu F, Jia Q X and Mitchell T E 1998 *J. Mater. Res.* **13** 2302
[30] Kanbayasi A 1976 *J. Phys. Soc. Japan* **41** 1876
[31] Noro Y and Miyahara S 1969 *J. Phys. Soc. Japan* **27** 518
[32] Narayan J, Tiwari P, Chen X, Singh J, Chowdhury R and Zheleva T 1992 *Appl. Phys. Lett.* **61** 1290